

## Accepted Manuscript

Title: Influence of calcination on metallic dispersion and support interactions for NiRu/TiO<sub>2</sub> catalyst in the hydrodeoxygenation of phenol

Authors: O.U. Valdés-Martínez, C.E. Santolalla-Vargas, V. Santes, J.A. de los Reyes, B. Pawelec, J.L.G. Fierro



PII: S0920-5861(18)31231-8  
DOI: <https://doi.org/10.1016/j.cattod.2018.11.007>  
Reference: CATTOD 11741

To appear in: *Catalysis Today*

Received date: 9 August 2018  
Revised date: 29 October 2018  
Accepted date: 2 November 2018

Please cite this article as: Valdés-Martínez OU, Santolalla-Vargas CE, Santes V, de los Reyes JA, Pawelec B, Fierro JLG, Influence of calcination on metallic dispersion and support interactions for NiRu/TiO<sub>2</sub> catalyst in the hydrodeoxygenation of phenol, *Catalysis Today* (2018), <https://doi.org/10.1016/j.cattod.2018.11.007>

This is a PDF file of an unedited manuscript that has been accepted for publication. As a service to our customers we are providing this early version of the manuscript. The manuscript will undergo copyediting, typesetting, and review of the resulting proof before it is published in its final form. Please note that during the production process errors may be discovered which could affect the content, and all legal disclaimers that apply to the journal pertain.

## **Influence of calcination on metallic dispersion and support interactions for NiRu/TiO<sub>2</sub> catalyst in the hydrodeoxygenation of phenol**

O.U. Valdés-Martínez <sup>a</sup>, C. E. Santolalla-Vargas <sup>b</sup>, V. Santes <sup>b</sup>, J. A. de los Reyes <sup>a\*</sup>, B. Pawelec <sup>c</sup> and J.L.G. Fierro <sup>c</sup>

<sup>a</sup> Área de Ingeniería Química. Universidad A. Metropolitana-Iztapalapa, Av. FFCC R. Atlixco 189 , 09340 Ciudad de México, México

<sup>b</sup> Departamento de Biociencias e Ingeniería, Centro Interdisciplinario de Investigaciones y Estudios sobre Medio Ambiente y Desarrollo (CIEMAD), Instituto Politécnico Nacional, C.P. 07340, Ciudad de México, México

<sup>c</sup> Instituto de Catálisis y Petroleoquímica, CSIC, C/ Marie Curie 2, Cantoblanco, E-28049, Madrid, Spain

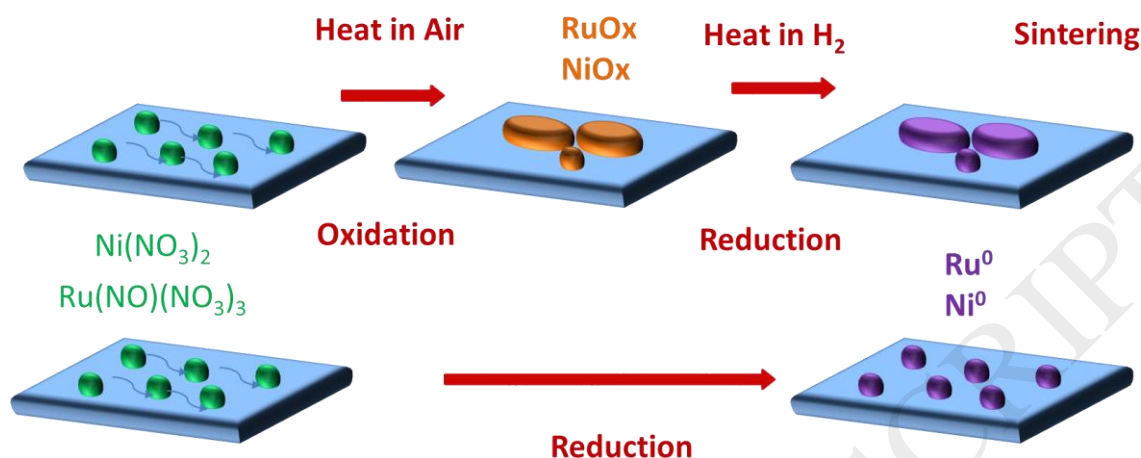
\* Corresponding author at:

Universidad A. Metropolitana, Área de Ingeniería Química, Av. FFCC R. Atlixco 186, Vicentina, 09340 Distrito Federal, México.

Tel: +52 5558044600 ext. 1247, Fax: +52 5556122479.

Email address: [jarh@xanum.uam.mx](mailto:jarh@xanum.uam.mx)

## Graphical Abstract



## Highlights

- The calcination procedure through the formation of metallic oxides induced less dispersed NiRu species.
- $\text{H}_2$  Chemisorption, benzene hydrogenation and HRTEM characterization pointed out that dispersion improved when catalyst was only dried and not calcined prior to reduction.
- Calcination induced sintering of metal particles leading to a decrease of HDO activity

## Abstract

Bio-oil upgrading by hydrotreatment has been considered as a renewable route for fuels production and potential substitutes for fossil oil distillates. Traditional hydrodesulfurization catalysts (sulfided CoMo and NiMo) used in petroleum refining have been evaluated in hydrodeoxygenation reactions with high selectivity to aromatics. However, significant deactivation has been commonly observed, due to the low sulfur content in bio-oil. Thus, the development of different active and stable catalytic materials is needed. In this regard, we have previously reported a synergetic effect between Ni and Ru bimetallic materials supported on  $\text{Al}_2\text{O}_3$ ,  $\text{TiO}_2$  and  $\text{ZrO}_2$  in phenol HDO with promising activity and selectivity results. In particular, materials supported  $\text{TiO}_2$  on displayed the

highest activities. Therefore, the aim of this work was to evaluate the effect of calcination on dispersion and metal-support interactions and their impact on activity and selectivity for NiRu/TiO<sub>2</sub> catalysts in HDO of phenol as a model compound for bio oil. Catalysts were characterized by hydrogen chemisorption, Temperature-programmed reduction, X-ray photoelectron spectroscopy, High resolution electron microscopy. Additionally, hydrogenation of benzene was used as a structure insensitive reaction in order to obtain more information about metallic dispersion. A highly active NiRu catalyst was obtained when calcination was avoided prior to reduction. The calcination procedure induced the formation of metallic oxides and it provoked less dispersed NiRu species as compared with catalysts without this previous treatment. On the contrary, the formation of metallic species from direct reduction of precursor salts contributed to produce highly dispersed species.

### **Keywords**

Nickel-Ruthenium; Hydrodeoxygenation; Phenol; Calcination; Dispersion

### **Introduction**

A continuous effort to mitigate the strong dependence of fossil fuels has motivated the research on new and alternative fuels derived from renewable resources. Lignocellulosic biomass can be transformed by fast pyrolysis into a product called bio-oil. This product has a high oxygen content that leads to chemical instability, immiscibility with fossil fuels and corrosion, preventing the direct application of this liquid in the transportation sector [1]. In this sense, upgrading bio-oils to liquid hydrocarbons is the clue in the development of a feasible route to obtain sustainable fuels from lignocellulose biomass [2].

Hydrodeoxygenation (HDO) is one of the main approaches to achieve this goal [3][4]. One relevant challenge in this process is to design an optimal catalyst, which should be active, stable and selective, allowing C-O bond scission with minimal H<sub>2</sub> consumption and carbon loss. The design of an adequate catalyst for HDO of bio-oil or model compounds requires the understanding of reaction routes. For example, two main parallel pathways have been proposed for phenol HDO[5]: (i) the direct deoxygenation (DDO), involves the CAR-O cleavage by hydrogenolysis to produce benzene; and (ii) the prehydrogenation of the aromatic ring (HYD) that leads to formation of cyclohexanol as an intermediate [6],

followed by dehydration of cyclohexanol to yield cyclohexene that is then hydrogenated to cyclohexane. Cyclohexene and methylcyclopentene could be then hydrogenated to the corresponding saturated compounds.

Due to the similarity of HDO with hydrodesulfurization (HDS), typical HDS catalyst (NiMoS, CoMoS supported on alumina) have been reported as active [6,7][8]. However, the lack of sulfur-containing compounds causes deactivation by the oxygen-sulfur exchange between sulfide active sites and oxygen in the mixture[9][6]. In this regard, the development of different active and stable catalytic materials is needed. Thus, metals like Fe, Cu and Ni have been widely studied in HDO. For instance, reduced nickel has shown to be highly active in aromatics hydrodeoxygenation [10]. Ni over oxidic supports exhibited the best performance in HDO in comparison with other metals, even as noble metals like Pt [11]. In a previous work we have reported a synergetic effect between Ni and Ru bimetallic materials supported on Al<sub>2</sub>O<sub>3</sub>, TiO<sub>2</sub> and ZrO<sub>2</sub> in phenol HDO with promising activity and selectivity results. [12]. For these materials, the presence of ruthenium enhanced nickel reducibility which was related to hydrogen dissociation of Ru<sup>0</sup> and a spillover effect with Ni [13], that could improve the hydrogen dissociation. This is needed for hydrogenation reactions that take place on metallic sites [9][14]. In addition to that, materials supported on TiO<sub>2</sub> have exhibited an outstanding performance as compared with other supports like SiO<sub>2</sub> and Al<sub>2</sub>O<sub>3</sub> [12][15]. Some authors have attributed this feature to the oxophilic nature of TiO<sub>2</sub> that induced the interaction of oxygen with the support, weakening the C-O bond and promoting the HDO reactions.[15][16].

Moreover, Ni-Ru bimetallic materials have been widely studied for other reactions, like CO methanation [17][13][18][19], CO<sub>2</sub> reforming [20][21] and hydrogen production [22][23][24]. Most of these Ni-Ru systems were calcined at temperature values above 773 K, leading to the formation of the respective metals oxides. On one hand, it is well known that calcination of Ni catalyst may induce strong interactions of the support with metal entities. These Ni species became more difficult to reduce as calcination temperature increased[25][26][27]. Furthermore, Louis et al. [28] indicated that calcination before reduction for Ni catalysts had an important influence on particle size distribution. These authors found that a reduction treatment without calcination induced the formation of

smaller particles than the reduction of calcined materials when Ni nitrate was used as precursor. On other hand, for Ru, other authors have reported that the reduction of impregnated ruthenium occurred at lower temperature when the precursor was not calcined as compared with the calcined solids. Also, reduction temperature and particle size increased with calcination temperature [29][30].

Nevertheless, the impact of direct reduction without calcination on HDO reactions has not been reported, to our knowledge, for Ni Ru bimetallic materials. It can be proposed that differences between both materials may be expected in terms of dispersion for the active phases (Ni and Ru) and metal support interactions [26][27][25][29][30]. Therefore, the aim of this work was to evaluate the effect of calcination on these parameters and their impact on activity and selectivity for NiRu/TiO<sub>2</sub> catalysts in HDO of phenol as a model compound for bio oil. Catalysts were characterized by hydrogen chemisorption, Temperature-programed reduction, X-ray photoelectron spectroscopy, High resolution electron microscopy. Additionally, hydrogenation of benzene was used as a structure insensitive reaction in order to obtain more information about metallic dispersion.

## 1. Experimental

### 1.1. Synthesis

TiO<sub>2</sub> was synthesized by sol-gel method as described elsewhere [31]. Specific area was  $S_{\text{BET}}=93 \text{ m}^2\text{g}^{-1}$ . XRD characterization revealed the presence of the anatase phase exclusively.

Bimetallic Ni - Ru catalysts were prepared by wet co-impregnation using an aqueous solution of nickel(II) nitrate hexahydrate (99.999 % Ni(NO<sub>3</sub>)<sub>2</sub>·6H<sub>2</sub>O; Aldrich), and ruthenium(III) nitrosyl nitrate (1.5 wt.-%Ru/vol., Ru(NO)(NO<sub>3</sub>)<sub>3</sub>; Aldrich) . Nominal metal loadings were 6 wt.-% Ni and 0.6 wt.-% Ru similar to the published by Tada et al [17]. Solids were dried at 393 K for 12 h then, one material was calcined at 773 K in static air while the other was not calcined to assess the influence of this process on the catalytic activity. Materials were reduced in-situ before reaction in a 60 ml/min H<sub>2</sub> flow at 773 K for calcined catalysts and 623 K for the uncalcined catalyst. Reduction temperatures were

selected according to TPR analyses and in order to avoid formation of metal titanate species in the uncalcined sample. It is highly possible that the higher reduction temperature used in calcined catalyst could also induce some sintering.

### 1.2. Hydrogen Chemisorption

Materials were reduced before analysis (623 K for *uncalcined* and 773 K for *calcined*). Once reduced and cooled, the reactor was evacuated with Ar. Chemisorption was carried out by pulses which were injected continuously until TCD signal do not vary indicating that hydrogen molecules covered metallic surface.

### 1.3. Hydrogenation of benzene

The hydrogenation of benzene was chosen as a structure insensitive reaction in order to obtain information about differences in metallic dispersion. Materials were reduced before experiments. Reaction was carried in a continuous down flow reactor at atmospheric pressure. Catalysts were reduced in situ before reaction at the same conditions used for phenol HDO (60 ml/min H<sub>2</sub> flow at 773 K for calcined catalysts and 623 K for the uncalcined catalyst), then reactor was cooled down to 323 K. Benzene was introduced to the reactor using H<sub>2</sub> stream as carrier through a saturator (WHSV = 2.4 × 10<sup>-3</sup> h<sup>-1</sup>). The reactor effluents were analyzed by a GC HP 5890 with a FID detector.

### 1.4. High-resolution transmission electron microscopy

High-resolution transmission electron microscopy (HRTEM) analyses for reduced catalysts were performed with a JEOL-2100F TEM (200 kV) instrument equipped with a Link ISIS micro-analysis system. Its resolution was 0.19 nm. The high-resolution images were captured digitally with a Gatan CCD digital camera. Samples were reduced under activation conditions as described previously and isolated under Ar atmosphere to avoid air contact. Before analyses, the reduced samples were finely ground, ultrasonically dispersed in ethanol and collected on a carbon-coated copper grid.

### 1.5. Temperature-programmed reduction

The temperature-programmed reduction (TPR) experiments for solids were carried out in an AMI-90 apparatus (Altamira) equipped with a thermal conductivity detector (TCD). About 50 mg of a sample were placed in a quartz sample cell (U-shaped) for each analysis. The samples were pretreated in situ at 373 K for 1h under Ar flow to remove physisorbed impurities. The reduction step was performed under a stream of (10 vol.-%) H<sub>2</sub>/Ar (50 cm<sup>3</sup>·min<sup>-1</sup>), with a heating rate of 10 K min<sup>-1</sup> up to 1073 K. A thermal conductivity detector was used to determine variations in the hydrogen composition of the output current. A moisture trap was used to prevent measurements interferences.

### 1.6. X-ray photoelectron spectroscopy

The X-ray photoelectron spectroscopy (XPS) studies for freshly reduced catalysts were performed in a VG scalab 200R spectrometer equipped with a hemispherical analyzer and Mg K $\alpha$  (h $\nu$ = 1253.6 eV) X-ray source. The calcined uncalcined samples were in situ reduced in H<sub>2</sub> at the mentioned conditions and then degassed (< 10<sup>-5</sup> Pa). All the data were acquired using monochromatic Mg K $\alpha$  radiation (1253.6 eV). The analyzed surface on the sample was 300 x 700 nm, and it allowed a representative characterization of the whole sample. The BE values for Ni 2p and Ru 3d spectra ( $\pm$ 0.2 eV) were determined by computer fitting using Casa XPS software of the measured spectra applying a Shirley background subtraction and Gaussian-Lorentzian decomposition parameters with 30/70 Gaussian/Lorentzian proportion. The BE were corrected taking the C 1s (248.4 eV) signal as a reference.

### 1.7. Temperature-programmed desorption of ammonia

The acidity for the catalysts was determined using the isothermal adsorption of NH<sub>3</sub> as obtained on a Micrometrics 2900 equipment. Before the analysis, the materials were in situ reduced in hydrogen under conditions described before. Then the solids were cooled and saturated with NH<sub>3</sub> at 373 K with a (5%) NH<sub>3</sub>/Ar flow. Desorption process was carried out between 273-923 K (10 K·min<sup>-1</sup>) in He flow. A Thermal Conductivity Detector was used to measure the NH<sub>3</sub> desorption. The area under desorption curve of the desorption profile was

used to quantify the acid sites. The acid site strength classification was based on the peak temperature range as follows: weak, 273K-523 K; medium, 523-673 K; and strong: 673-723 K; according to previously published results [12].

### 1.8. Hydrodeoxygenation of phenol

The hydrodeoxygenation of phenol was carried out in a high pressure laboratory scale set up equipped with a down flow fixed bed catalytic reactor. For each experiment ca. 0.15 g of catalyst (particle diameter 0.25–0.30 mm) were mixed with SiC (3:1) diameter 0.25 mm). The catalyst was reduced in situ at 623 K (for *uncalcined*) and 773 K (for *calcined*) 2 h in H<sub>2</sub> under atmospheric pressure. The temperature was selected after TPR experiment, as the temperature were metal was expected to be completely reduced. After reduction, H<sub>2</sub> pressure was increased to the desired value (3.0 MP), and the catalytic bed was heated up to the temperature of the HDO reaction (593 K). The liquid feed (2 vol% of phenol dissolved in dodecane) was injected by a high-pressure HPLC Knauer pump (WHSV = 2.57 h<sup>-1</sup>) into a hydrogen stream (40 mL min<sup>-1</sup>). The reactor effluents were condensed, and liquid samples were analyzed by a GC Agilent 6890A with a FID detector.

### 1.9. TGA

The amount of deposited coke on the catalysts tested in HDO of phenol reaction was determined with a thermogravimetric TGA/SDTA851 equipment (Mettler Toledo), measuring the weight change in the coked catalysts during oxidation. Each sample (ca. 30 mg) was previously heated in inert atmosphere remove the volatile compounds up to 773 K for 1 h in N<sub>2</sub> (10 K min<sup>-1</sup>; 200 mL min<sup>-1</sup> flow-rate). Once the sample was cooled to 300 K (5 K min<sup>-1</sup>) burning of coke was carried out by raising sample temperature to a final temperature of 1073 K at a rate of 10 K min<sup>-1</sup> in a 20% O<sub>2</sub>/N<sub>2</sub> gas mixture (50 mL min<sup>-1</sup>).

## 2. Results and discussion

### 2.1. Hydrogen Chemisorption

Hydrogen chemisorption was performed to compare exposed metallic areas for *calcined* and *uncalcined* bimetallic NiRu catalysts supported on TiO<sub>2</sub>. **Table 1** gives the amount of

chemisorbed hydrogen per gram of catalyst. It was observed that the amount of gas retained by the *calcined* solid was 4.2 H<sub>2</sub> μmol/g of catalyst, while for the *uncalcined* sample was 45.8 H<sub>2</sub> μmol/g of catalyst (ca. 9 times). This fact indicated that calcination affected considerably the metallic dispersion.

## 2.2. Hydrogenation of benzene

Benzene hydrogenation was carried out as a structure insensitive reaction in order to obtain more information about differences in metallic dispersion. Since hydrogenation reactions only take place on metallic sites[32], differences in hydrogenation rates are only related to differences in metallic dispersion for catalyst with identical metal loadings. **Table 1** gives reaction rates for benzene hydrogenation for both NiRu catalysts. *Uncalcined* catalyst exhibited a 8 fold higher activity than that for the *calcined* one, in good agreement with the H<sub>2</sub> chemisorption results. These results clearly indicated that metallic particles in *uncalcined* NiRu/TiO<sub>2</sub> showed higher dispersed than in the *calcined* NiRu/TiO<sub>2</sub>.

## 2.3. High-resolution transmission electron microscopy

To explore the effect of calcination on the morphology and surface distribution for metallic crystallites, high-resolution images for *uncalcined* and *calcined* NiRu/TiO<sub>2</sub> catalysts were analyzed (**Figure 1**). In general, arbitrary agglomerated crystalline particles were observed. From Fast Fourier Transform (FFT) performed on the images, these particles presented mainly *d*-spacing of 3.52 and 1.89 Å, that could be indexed to the (101) and (200) crystalline planes on the *anatase*-TiO<sub>2</sub> lattice. The presence of Ni and Ru was confirmed by EDX and indexation of crystalline metal particles in HRTEM images. In this case, small particles with *d*-spacing 2.04 Å were indexed to the (111) crystalline plane of face-centered cubic Ni lattice (*cubic*-Ni; JCPD-ICDD-PDF: 004-0850). Meanwhile, the *d*-spacing of 2.09 and 2.3 nm could be indexed as (101) and (100) crystalline planes of hexagonal close-packed Ru lattice (*hexagonal*-Ru; JCPD-ICDD-PDF: 006-0663). **Figure 1** shows the particle size distributions for the *uncalcined* and *calcined* solids respectively,.It was confirmed that calcination influenced strongly metallic dispersion. Therefore, these metallic particles for *uncalcined* catalyst were almost 4.6 times smaller than those observed on the *calcined* one. Taking into account that the statistic calculation of the particle size is based

on the information obtained from a large number of TEM images having low resolution. Thus, we assume that the particle size obtained correspond mainly to metallic Ni phase.

It was not possible to identify the formation of bimetallic clusters or zones of close contact between Ni and Ru by using this technique, as previously reported by others[17]. As a consequence, it is impossible to speculate on the possible influence of Ru on the catalyst activity.

#### 2.4. Temperature-programmed reduction

**Figure 2** shows the reduction profiles for *uncalcined* and *calcined* samples. The TPR profile for *calcined* NiRu/TiO<sub>2</sub> catalysts (**Figure 2 a**) exhibited a sharp peak centered at 419 K. It can be assigned to the RuO<sub>2</sub> → Ru<sup>0</sup> reduction in good agreement with the literature[19][33]. The peak located at 680 K was assigned to NiO<sub>x</sub> reduction, whereas the reduction process between 470-570 K could be related to the reduction of bimetallic species[19]. Above 780 K, all reducible species were transformed into their metallic state, since reduction before reaction was carried out at 723 K. Thus, one may assume that Ni<sup>0</sup> and Ru<sup>0</sup> species were present during reaction. For the *uncalcined*-NiRu sample (**Figure 2 b**), a sharp reduction peak at 483 K can be assigned to the reduction of Ru and Ni in the impregnated ruthenium nitrosyl complex (Ru<sup>3+</sup> → Ru<sup>0</sup>) [34] and nickel hexahydrate complex (Ni<sup>2+</sup> → Ni<sup>0</sup>) [35][36] occurring simultaneously. The sharp shape of the reduction peak suggested a uniform distribution of metal entities. Furthermore, the next low intense peak was associated with a reduction of Ni complex in low interaction with the support[34][35]. Pre-reduction for reaction was performed at 623 K, thus the active phases were also Ni<sup>0</sup> and Ru<sup>0</sup>. Based on the form and position of peaks, we assume that calcination induced stronger metal support interaction than the drying, which promoted particle growth, as reported by other authors[26][27][25].

#### 2.5. X-ray photoelectron spectroscopy

**Figure 3** gives Ni 2p<sub>1/2</sub> and Ni 2p<sub>3/2</sub> XPS levels spectra for a) *calcined* and b) *uncalcined* samples. Both spectra are composed of two adjacent bands with a maximum at 851 eV and 855 eV and their satellites. Appropriate decomposition was carried out for the spectra,

considering bands associated with  $\text{Ni}^0$  and  $\text{Ni}^{2+}$  ( $\approx 852.2$  eV and  $\approx 855$  eV respectively). Notable differences related with the amounts of  $\text{Ni}^0$  and  $\text{Ni}^{2+}$  can be observed between both catalysts (**Table 2**). For the *calcined* catalyst, 77% of Ni in the solid was reduced while 23 % was at the oxidic state. Thus, the reduction conditions were not optimal to reduce completely NiO as produced from calcination. Besides, only 60% of Ni was found in metallic state and 40% as not reduced Ni species for the uncalcined sample. The reduction conditions neither were enough for the total reduction of Ni. **Table 2** gives XPS results for the Ru 3d level. For both materials, the XPS results for the Ru 3d showed that this metal was completely reduced after treatments.

## 2.6. Temperature-programmed desorption

**Table 3** gives the weak medium and strong acid sites densities as determined from  $\text{NH}_3$  TPD experiments. This table shows that the total acid sites concentration was similar for both materials. However the *uncalcined* solid exhibited 26% more weak and medium strength acid sites according to the strength classification based on temperature desorption range (273K-523 K; medium, 523-673 K; and strong: 673-723 K). A decrease of acidity induced by calcination at high temperatures has been widely reported [37][27]. The higher concentration of acid sites for the uncalcined sample can be explained in terms of remaining OH groups on the carrier after impregnation, and the presence of  $\text{NiO}_x$  species originated from the precursors reduction process. Calcination of the catalyst, as generally accepted, promotes the dehydroxylation of the support. In addition to the improved dispersion, the higher weak and medium acid site density may also beneficiate the HDO activity. These sites are involved in dehydration reactions needed to the cleavage of oxygen as water. In this regard, a linear correlation between acid sites density and HDO reaction rate was reported before [12][38].

In this work the uncalcined catalyst reduced at 773 K exhibited a larger amount of medium strength acid sites than its calcined counterpart reduced at 623 K. For the strong strength acid sites, the contrary trend occurs. This is expected because the calcination of NiRu/TiO<sub>2</sub> sample led probably to formation of the metal titanate species, which were not formed by direct reduction of the uncalcined catalyst.

## 2.7. Hydrodeoxygenation of phenol

**Table 4** gives the phenol hydrodeoxygenation activity and selectivity for *calcined* and *uncalcined* catalyst. The HDO reaction rate for the *calcined* catalyst was  $17.8 \mu\text{mol of phenol} \cdot \text{g of catalyst}^{-1} \cdot \text{s}^{-1}$  while for the *uncalcined* was  $149 \mu\text{mol of phenol} \cdot \text{catalyst}^{-1} \cdot \text{s}^{-1}$  (8.3 higher than the calcined one). Regarding HDO selectivities, the main products identified by GC were cyclohexane and methylcyclopentane, with a small production of benzene. **Table 4** gives the HYD to DDO ratio. It can be seen that the HYD route was preferred over DDO for both catalysts. In these materials phenol activation may occur via a heterolytic dissociation of the O–H bond when phenol is absorbed on a surface oxygen site of support, near to a metallic site. This site stabilizes the phenoxide ion. Consequently, the phenoxide ion will be in close interaction with the metal where the hydrogen is free to react[11]. After hydrogenation take place, an OH group of cyclohexanol may be easily dehydrated to yield cyclohexene molecule. It is commonly accepted that dehydration of alcohols occurs on acid sites. Therefore, a high density of acid sites may induce a fast dehydration of cyclohexanol[11][12]. In this work there was not correlation between the acidities of the pre-reduced catalysts samples and their HYD/DDO selectivities ratio calculated at the same phenol conversion. This is probably because the larger amount of medium strength acid sites of the uncalcined sample was compensated by the effect of the larger amount of strong acid sites of its calcined counterpart (Table 3). The absence of the correlation between the catalysts acidities and HDO/DDO selectivities ratio was reported previously[12].

Since catalysts were reduced before reaction, metallic Ni and Ru were the active phases for both materials.  $\text{Ni}^0$  and  $\text{Ru}^0$  were obtained by the reduction of NiO and RuO for *calcined* catalyst, as a results of calcination respectively. Besides, for *uncalcined* catalyst metallic Ni and Ru were produced by the reduction of the residual impregnated species from  $\text{Ni}(\text{NO}_3)_2$  and  $\text{Ru}(\text{NO})(\text{NO}_3)_3$ . In this regard, the main differences between both material may be dispersion of the same actives phases (Ni and Ru) and metal support interaction.

Additionally, particle growth by high temperature treatment and strong metal support interaction as a consequence of calcination may explain the lower

activity[26][27][25][29][30]. Also, uncalcined Ru materials were reported as more active previously[30].

Table 4 present also the estimated TOF values for both catalysts, the difference between them may be indicative than metal dispersion is not enough to explain the main impact of calcination process. However experimental errors should be taken into account when comparing both values. It should be considered that Ru content in the calcined sample could be slightly lower than in the uncalcined sample, since Ru precursors could be oxidized at temperatures up to 673 K to a volatile form such as RuO<sub>4</sub> [39]. Additionally, the larger density of acid sites in the uncalcined catalyst could contribute to a higher catalytic activity for this sample as compared with the calcined one. . Current research is been carried out to rule out this possibility.

## 2.8.TGA

After catalyst drying, a burning of coke was carried out by raising sample temperature to a final value of 1073 K at a rate of 10 K min<sup>-1</sup> in a 20% O<sub>2</sub>/N<sub>2</sub> gas mixture. This technique confirmed that the main catalyst deactivation in this reaction was due to deposition of carbonaceous residues/coke on the catalyst surface. Therefore, one might expect that the availability of hydrogen on metal sites should be lower. The weight change during oxidation of the spent catalysts in a 20% O<sub>2</sub>/N<sub>2</sub> mixture (TGA profiles) is shown in **Figure 4** . At low temperature region, for all catalysts the weight gain is observed due to oxidation of metallic Ni( Ru) to Ni<sup>2+</sup>(Ru<sup>2+</sup>). At high temperature region, the weight loss is due to the gasification of carbon. The percentages of total mass gain and loss corresponding to oxidation of metal species and coke, respectively, are shown in **Table 5**.

As seen in **Figure 4**, there is some change in the intensity and position of the peaks for all samples induced by the different size of the metal particles and type of support. In good agreement with study by Luo et al.[40], for *calcined* NiRu/TiO<sub>2</sub> catalyst, the removal of carbon filamentous occurs at temperature above 943 K. Noticeably, the *uncalcined* NiRu/TiO<sub>2</sub> exhibits totally different TG profile: removal of carbon occurs at much lower temperature (about 573 K) and occurs in two steps indicating the formation of two types of coke and/or its different location on the catalyst surface[41] The catalyst regeneration by

oxidation is easy because of a low amount of coke formed and its more favourable composition. Considering the study by Ibáñez et al. [41] we assume that coke formed has aliphatic nature (non aromatic nature).

Summarizing, we conclude that the morphology of the carbon is essentially affected by the catalyst pre-treatment (drying vs. calcination) and the size of the Ni/Ru particles. However, the same amount of coke was formed on the calcined and non-calcined samples. Pre-reduction of the *uncalcined* catalysts was more favorable to the catalyst stability because formed coke, which could be more easily removed by the catalyst oxidation at much lower temperature than in case of the calcined sample.

### 3. Conclusions

Calcination of NiRu catalyst supported on TiO<sub>2</sub> induced sintering of metal particles and dispersion was significantly lower when compared with solids not calcined prior to reduction. Calcination also induced a decrease of weak and medium acid sites. Both effects influenced strongly higher HDO activities (8.3) for uncalcined material as compared with the calcined solid. Finally, TGA showed that prereduction of uncalcined catalyst was more favorable for the catalyst stability because formed coke could be easily removed by catalyst oxidation at much lower temperature than in case of the calcined catalyst.

### 4. Acknowledgements

The authors acknowledge financial support from CONACYT-México (Grant 237857). We also thank Instituto Politécnico Nacional (Proyecto SIP 20181105).

## 5. References

- [1] G.W. Huber, S. Iborra, A. Corma, Synthesis of Transportation Fuels from Biomass: Chemistry, Catalysts, and Engineering, *Chem. Rev.* 106 (2006) 4044–4098. doi:10.1021/cr068360d.
- [2] M. Stöcker, Biofuels and biomass-to-liquid fuels in the biorefinery: Catalytic conversion of lignocellulosic biomass using porous materials, *Angew. Chemie - Int. Ed.* 47 (2008) 9200–9211. doi:10.1002/anie.200801476.
- [3] C. Zhao, Y. Kou, A.A. Lemonidou, X. Li, J.A. Lercher, Highly selective catalytic conversion of phenolic bio-oil to alkanes, *Angew. Chemie - Int. Ed.* 48 (2009) 3987–3990. doi:10.1002/anie.200900404.
- [4] A. Gutierrez, R.K. Kaila, M.L. Honkela, R. Slioor, A.O.I. Krause, Hydrodeoxygenation of guaiacol on noble metal catalysts, *Catal. Today.* 147 (2009) 239–246. doi:10.1016/J.CATTOD.2008.10.037.
- [5] F.E. Massoth, P. Politzer, M.C. Concha, J.S. Murray, J. Jakowski, J. Simons, Catalytic Hydrodeoxygenation of Methyl-Substituted Phenols: Correlations of Kinetic Parameters with Molecular Properties, *J. Phys. Chem. B.* 110 (2006) 14283–14291. doi:10.1021/jp057332g.
- [6] V.N. Bui, D. Laurenti, P. Afanasiev, C. Geantet, Hydrodeoxygenation of guaiacol with CoMo catalysts. Part I: Promoting effect of cobalt on HDO selectivity and activity, *Appl. Catal. B Environ.* 101 (2011) 239–245. doi:10.1016/J.APCATB.2010.10.025.
- [7] A. Popov, E. Kondratieva, L. Mariey, J.M. Goupil, J. El Fallah, J.-P. Gilson, A. Travert, F. Maugé, Bio-oil hydrodeoxygenation: Adsorption of phenolic compounds on sulfided (Co)Mo catalysts, *J. Catal.* 297 (2013) 176–186. doi:10.1016/J.JCAT.2012.10.005.
- [8] D.C. Elliott, Historical Developments in Hydroprocessing Bio-oils, *Energy & Fuels.* 21 (2007) 1792–1815. doi:10.1021/ef070044u.
- [9] E. Furimsky, Catalytic hydrodeoxygenation, *Appl. Catal. A Gen.* 199 (2000) 147–190. doi:10.1016/S0926-860X(99)00555-4.
- [10] P.M. Mortensen, J.D. Grunwaldt, P.A. Jensen, A.D. Jensen, Influence on nickel particle size on the hydrodeoxygenation of phenol over Ni/SiO<sub>2</sub>, *Catal. Today.* 259 (2016) 277–284. doi:10.1016/j.cattod.2015.08.022.
- [11] P.M. Mortensen, J.D. Grunwaldt, P.A. Jensen, A.D. Jensen, Screening of catalysts for hydrodeoxygenation of phenol as a model compound for bio-oil, *ACS Catal.* 3 (2013) 1774–1785. doi:10.1021/cs400266e.
- [12] O.U. Valdés-Martínez, V.A. Suárez-Toriello, J.A. d. los Reyes, B. Pawelec, J.L.G. Fierro, Support effect and metals interactions for NiRu/Al<sub>2</sub>O<sub>3</sub>, TiO<sub>2</sub> and ZrO<sub>2</sub> catalysts in the hydrodeoxygenation of phenol, *Catal. Today.* 296 (2017) 219–227. doi:10.1016/j.cattod.2017.04.007.
- [13] S. Tada, D. Minori, F. Otsuka, R. Kikuchi, K. Osada, K. Akiyama, S. Satokawa, Effect of Ru and Ni ratio on selective CO methanation over Ru-Ni/TiO<sub>2</sub>, *Fuel.* 129 (2014) 219–224. doi:10.1016/j.fuel.2014.03.069.
- [14] X. Zhu, L. Nie, L.L. Lobban, R.G. Mallinson, D.E. Resasco, Efficient Conversion of m-Cresol to Aromatics on a Bifunctional Pt / HBeta Catalyst, (2014).
- [15] P.M. de Souza, R.C. Rabelo-Neto, L.E.P. Borges, G. Jacobs, B.H. Davis, D.E. Resasco, F.B. Noronha, Hydrodeoxygenation of Phenol over Pd Catalysts. Effect of Support on Reaction Mechanism and Catalyst Deactivation, *ACS Catal.* 7 (2017) 2058–2073. doi:10.1021/acscatal.6b02022.
- [16] P.M. De Souza, L. Nie, L.E.P. Borges, F.B. Noronha, D.E. Resasco, Role of oxophilic supports in the selective hydrodeoxygenation of m-cresol on Pd catalysts, *Catal. Letters.* 144

- (2014) 2005–2011. doi:10.1007/s10562-014-1337-y.
- [17] S. Tada, R. Kikuchi, K. Wada, K. Osada, K. Akiyama, S. Satokawa, Y. Kawashima, Long-term durability of Ni/TiO<sub>2</sub> and Ru–Ni/TiO<sub>2</sub> catalysts for selective CO methanation, *J. Power Sources*. 264 (2014) 59–66. doi:10.1016/J.JPOWSOUR.2014.04.075.
- [18] S. Tada, R. Kikuchi, A. Takagaki, T. Sugawara, S. Ted Oyama, S. Satokawa, Effect of metal addition to Ru/TiO<sub>2</sub> catalyst on selective CO methanation, *Catal. Today*. 232 (2014) 16–21. doi:10.1016/j.cattod.2013.09.048.
- [19] S. Tada, R. Kikuchi, A. Takagaki, T. Sugawara, S.T. Oyama, K. Urasaki, S. Satokawa, Study of RuNi/TiO<sub>2</sub> catalysts for selective CO methanation, *Appl. Catal. B Environ*. 140–141 (2013) 258–264. doi:10.1016/j.apcatb.2013.04.024.
- [20] C. Crisafulli, S. Scire, R. Maggiore, S. Minico, S. Galvagno, CO<sub>2</sub> reforming of methane over Ni – Ru and Ni – Pd bimetallic catalysts, *Catal. Letters*. 59 (1999) 21–26.
- [21] C. Crisafulli, S. Scirè, S. Minicò, L. Solarino, Ni – Ru bimetallic catalysts for the CO<sub>2</sub> reforming of methane, *Appl. Catal.* 225 (2002) 1–9. doi:10.1016/S0926-860X(01)00585-3.
- [22] E. Salehi, F.S. Azad, T. Harding, J. Abedi, Production of hydrogen by steam reforming of bio-oil over Ni/Al<sub>2</sub>O<sub>3</sub> catalysts: Effect of addition of promoter and preparation procedure, *Fuel Process. Technol.* 92 (2011) 2203–2210. doi:10.1016/j.fuproc.2011.07.002.
- [23] V. Modafferi, G. Panzera, V. Baglio, F. Frusteri, P.L. Antonucci, Propane reforming on Ni–Ru/GDC catalyst: H<sub>2</sub> production for IT-SOFCs under SR and ATR conditions, *Appl. Catal. A Gen.* 334 (2008) 1–9. doi:10.1016/j.apcata.2007.10.006.
- [24] S.C. Baek, K.W. Jun, Y.J. Lee, J.D. Kim, D.Y. Park, K.Y. Lee, Ru/Ni/MgAl<sub>2</sub>O<sub>4</sub> catalysts for steam reforming of methane: Effects of Ru content on self-activation property, *Res. Chem. Intermed.* 38 (2012) 1225–1236. doi:10.1007/s11164-011-0462-0.
- [25] F.W. Chang, M.S. Kuo, M.T. Tsay, M.C. Hsieh, Effect of calcination temperature on catalyst reducibility and hydrogenation reactivity in rice husk ash-alumina supported nickel systems, *J. Chem. Technol. Biotechnol.* 79 (2004) 691–699. doi:10.1002/jctb.1029.
- [26] J.G. Seo, M.H. Youn, J.S. Chung, I.K. Song, Effect of calcination temperature of mesoporous nickel-alumina catalysts on their catalytic performance in hydrogen production by steam reforming of liquefied natural gas (LNG), *J. Ind. Eng. Chem.* 16 (2010) 795–799. doi:10.1016/j.jiec.2010.05.010.
- [27] L. Smoláková, M. Kout, E. Koudelková, L. Čapek, Effect of Calcination Temperature on the Structure and Catalytic Performance of the Ni/Al<sub>2</sub>O<sub>3</sub> and Ni–Ce/Al<sub>2</sub>O<sub>3</sub> Catalysts in Oxidative Dehydrogenation of Ethane, *Ind. Eng. Chem. Res.* 54 (2015) 12730–12740. doi:10.1021/acs.iecr.5b03425.
- [28] C. Louis, Z.X. Cheng, M. Che, Characterization of nickel/silica catalysts during impregnation and further thermal activation treatment leading to metal particles, *J. Phys. Chem.* 97 (1993) 5703–5712. doi:10.1021/j100123a040.
- [29] T. LI, S. WANG, D. GAO, S. WANG, Effect of support calcination temperature on the catalytic properties of Ru/Ce<sub>0.8</sub>Zr<sub>0.2</sub>O<sub>2</sub> for methanation of carbon dioxide, *J. Fuel Chem. Technol.* 42 (2014) 1440–1446. doi:10.1016/S1872-5813(15)60001-9.
- [30] L. Zhao, J. Zhou, H. Chen, M. Zhang, Z. Sui, X. Zhou, Carbon nanofibers supported Ru catalyst for sorbitol hydrogenolysis to glycols: Effect of calcination, *Korean J. Chem. Eng.* 27 (2010) 1412–1418. doi:10.1007/s11814-010-0257-9.
- [31] S. Núñez, J. Escobar, A. Vázquez, J.A. de los Reyes, M. Hernández-Barrera, 4,6-Dimethyl-dibenzothiophene conversion over Al<sub>2</sub>O<sub>3</sub>–TiO<sub>2</sub>-supported noble metal catalysts, *Mater. Chem. Phys.* 126 (2011) 237–247. doi:10.1016/J.MATCHEMPHYS.2010.11.032.
- [32] F. Fajardie, J.-F. Tempère, G. Djèga-Mariadassou, G. Blanchard, Benzene Hydrogenation as a Tool for the Determination of the Percentage of Metal Exposed on Low Loaded Ceria Supported Rhodium Catalysts, *J. Catal.* 163 (1996) 77–86. doi:10.1006/JCAT.1996.0306.
- [33] I.M. Leo, M.L. Granados, J.L.G. Fierro, R. Mariscal, Sorbitol hydrogenolysis to glycols by supported ruthenium catalysts, *Chinese J. Catal.* 35 (2014) 614–621. doi:10.1016/S1872-

- 2067(14)60086-3.
- [34] A.M. Serrano-Sánchez, P. Steltenpohl, M.P. González-Marcos, J.A. González-Marcos, J.R. González-Velasco, Evaluation of the oxidizing potential of Ru and Ru-Pt/ZrO<sub>2</sub> catalysts for NO oxidation in the presence of C<sub>3</sub>H<sub>6</sub> and O<sub>2</sub>, *Chem. Pap.* 58 (2004) 41–47.
- [35] C.E. Santolalla-Vargas, V.A. Suárez Toriello, J.A. de los Reyes, D.K. Cromwell, B. Pawelec, J.L.G. Fierro, Effects of pH and chelating agent on the NiWS phase formation in NiW/ $\gamma$ -Al<sub>2</sub>O<sub>3</sub> HDS catalysts, *Mater. Chem. Phys.* 166 (2015) 105–115. doi:10.1016/J.MATCHEMPHYS.2015.09.033.
- [36] V.A. Suárez-Toriello, C.E. Santolalla-Vargas, J.A. de los Reyes, A. Vázquez-Zavala, M. Vrinat, C. Geantet, Influence of the solution pH in impregnation with citric acid and activity of Ni/W/Al<sub>2</sub>O<sub>3</sub> catalysts, *J. Mol. Catal. A Chem.* 404–405 (2015) 36–46. doi:10.1016/J.MOLCATA.2015.04.005.
- [37] H. Xu, M. Sun, S. Liu, Y. Li, J. Wang, Y. Chen, Effect of the calcination temperature of cerium-zirconium mixed oxides on the structure and catalytic performance of WO<sub>3</sub>/CeZrO<sub>2</sub> monolithic catalyst for selective catalytic reduction of NO<sub>x</sub> with NH<sub>3</sub>, *RSC Adv.* 7 (2017) 24177–24187. doi:10.1039/C7RA03054A.
- [38] Y. Elkasabi, C.A. Mullen, A.L.M.T. Pighinelli, A.A. Boateng, Hydrodeoxygenation of fast-pyrolysis bio-oils from various feedstocks using carbon-supported catalysts, *Fuel Process. Technol.* 123 (2014) 11–18. doi:10.1016/J.FUPROC.2014.01.039.
- [39] P.W. Cains, K.C. Yewer, S. Waring, Volatilization of Ruthenium, Caesium and Technetium from Nitrate Systems in Nuclear Fuel Processing and Waste Solidification, *Radiochim. Acta.* 56 (1992) 99–104. doi:10.1524/ract.1992.56.2.99.
- [40] J.Z. Luo, Z.L. Yu, C.F. Ng, C.T. Au, CO<sub>2</sub>/CH<sub>4</sub> Reforming over Ni–La<sub>2</sub>O<sub>3</sub>/5A: An Investigation on Carbon Deposition and Reaction Steps, *J. Catal.* 194 (2000) 198–210. doi:10.1006/JCAT.2000.2941.
- [41] M. Ibáñez, M. Artetxe, G. Lopez, G. Elordi, J. Bilbao, M. Olazar, P. Castaño, Identification of the coke deposited on an HZSM-5 zeolite catalyst during the sequenced pyrolysis–cracking of HDPE, *Appl. Catal. B Environ.* 148–149 (2014) 436–445. doi:10.1016/J.APCATB.2013.11.023.

**Figure 1.** HRTEM images and particle size distribution for NiRu/TiO<sub>2</sub> catalysts a) *calcined* and b) *uncalcined*

**Figure 2.** TPR profiles for NiRu/TiO<sub>2</sub> catalysts a) *calcined* and b) *uncalcined*

**Figure 3.** XPS spectra comparison for reduced NiRu/TiO<sub>2</sub> catalysts a) *calcined* and b) *uncalcined*

**Figure 5.** TG profiles for the reduced NiRu/TiO<sub>2</sub> a) *calcined* and b) *uncalcined* catalysts after catalytic evaluation in the HDO of phenol.

**Figure 1**

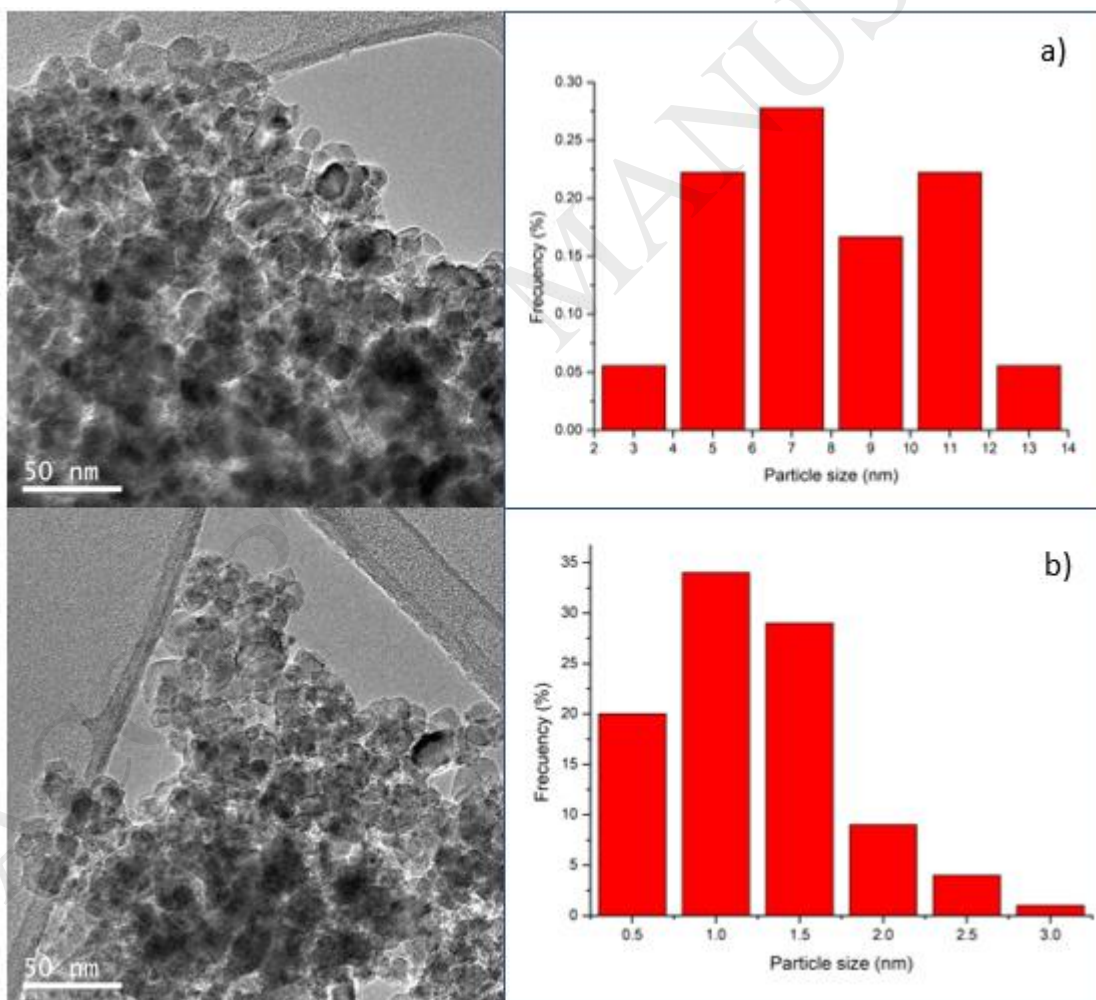


**Figure 2**

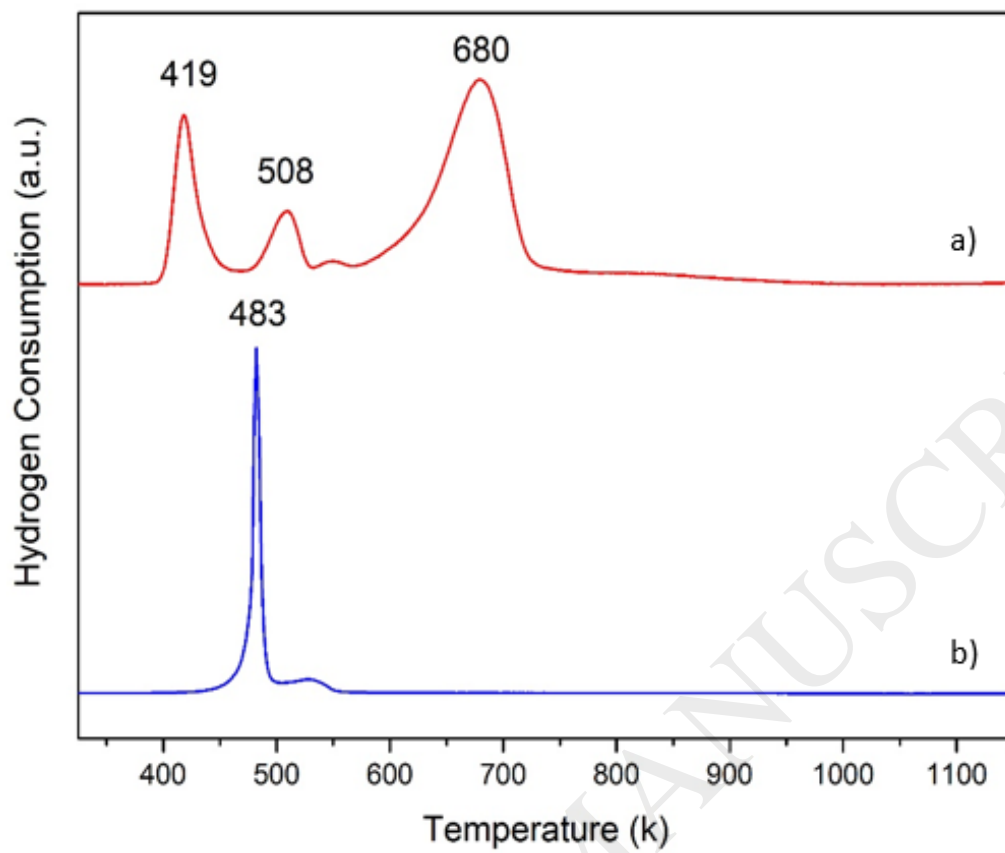


Figure 3

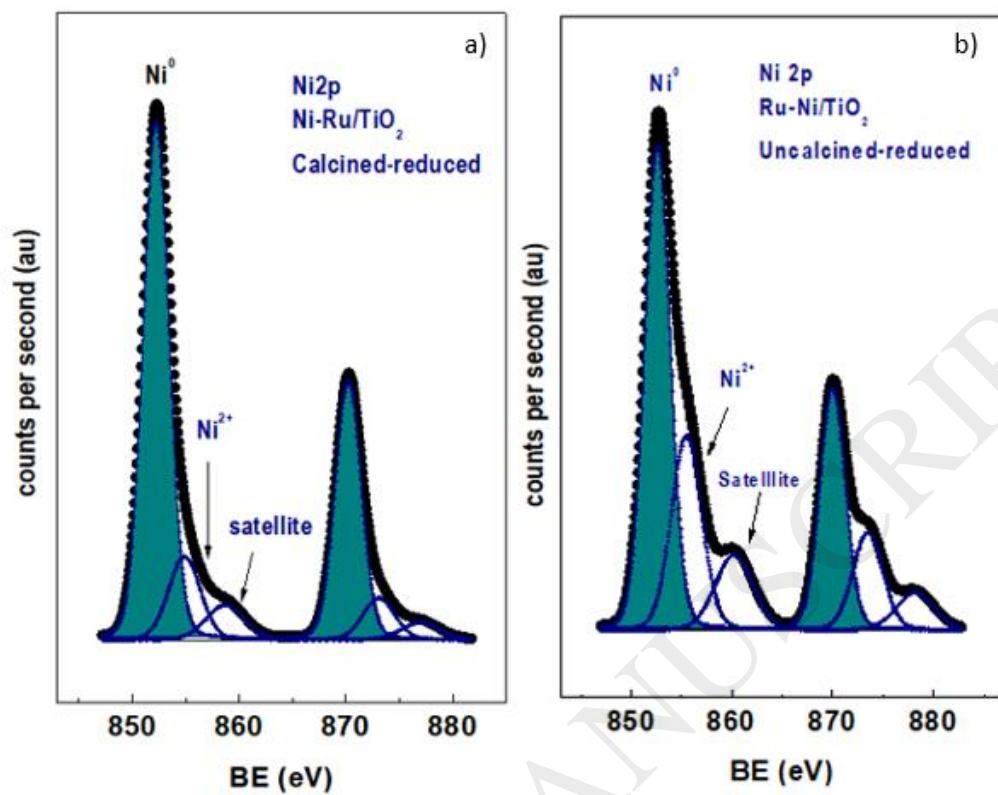
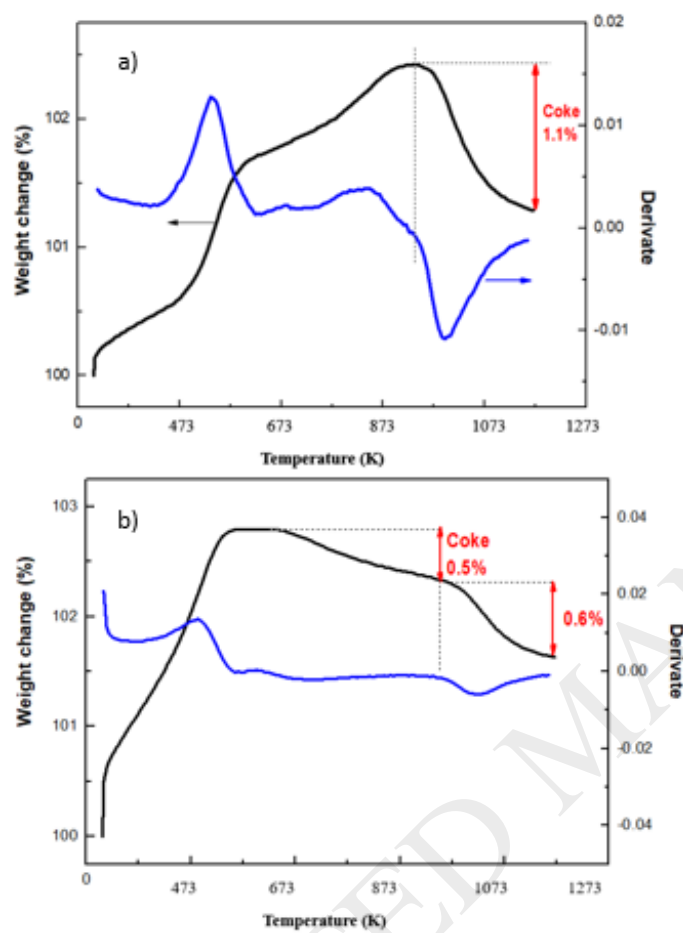


Figure 4



**Table 1** H<sub>2</sub> Chemisorption results, benzene hydrogenation rates and calculated average particle size for reduced NiRu TiO<sub>2</sub> catalysts

Catalyst	NiRu/TiO <sub>2</sub> (calcined) <sup>a</sup>	NiRu/TiO <sub>2</sub> (uncalcined) <sup>b</sup>
H <sub>2</sub> chemisorbed H <sub>2</sub> [ $\mu\text{mol H}_2/\text{g of catalyst}$ ]	4.2	45.8
Benzene HYD Rate <sup>c</sup> [ $\mu\text{mol Benzene}/\text{g of catalyst s}$ ]	1.17	8.3
Average particle size (nm) <sup>d</sup>	9.9	2.14

<sup>a</sup> Pre-reduced at 773 K<sup>b</sup> Pre-reduced at 623 K<sup>c</sup> Calculated at steady-state conditions<sup>d</sup> Estimated by HRTEM**Table 2** XPS binding energies and relative percentage of species for reduced NiRu/TiO<sub>2</sub> catalysts.

Catalyst	NiRu/TiO <sub>2</sub> (calcined) <sup>a</sup>	NiRu/TiO <sub>2</sub> (uncalcined) <sup>b</sup>
Ni 2p <sub>3/2</sub> Ni <sup>0</sup> (%)	852.2 eV (77)	852.6 eV (60)
Ni 2p <sub>3/2</sub> Ni <sup>2+</sup> (%)	854.9 eV (23)	855.5 eV (40)
Ru 3d <sub>5/2</sub> Ru <sup>0</sup>	280.1 eV(100)	280.1 eV(100)

<sup>a</sup> After reduction at 773 K<sup>b</sup> After reduction at 623 K**Table 3.** Acid sites density for reduced NiRu/ TiO<sub>2</sub> catalysts

Catalyst	Amount of acid sites ( $\mu\text{mol NH}_3 \cdot \text{g}_{\text{cat}}$ )	
	NiRu/TiO <sub>2</sub> (calcined) <sup>a</sup>	NiRu/TiO <sub>2</sub> (uncalcined) <sup>b</sup>
Weak (273 K-523K)	58	64
Medium (523 K-673 K)	45	67
Strong (> 673 K)	19	6

<sup>a</sup> After reduction at 773 K<sup>b</sup> After reduction at 623 K

**Table 4** Catalytic activity and selectivity of reduced NiRu /TiO<sub>2</sub> Catalyst

<b>HDO od Phenol</b>	NiRu/TiO <sub>2</sub> (calcined) <sup>a</sup>	NiRu/TiO <sub>2</sub> (uncalcined) <sup>b</sup>
Phenol HDO Rate <sup>c</sup> [ $\mu\text{mol/g}$ of catalyst s]	17.8	149
Selectivity <sup>d</sup> (HYD/DDO)	4.59	4.61
TOF [ $\text{s}^{-1}$ ]	0.83	0.68

<sup>a</sup> After reduction at 773 K<sup>b</sup> After reduction at 623 K<sup>c</sup> Obtained at steady-state conditions<sup>d</sup> Calculated at same phenol conversion(70%)**Table 5** Percentages of mass gain and loss corresponding to oxidation of metal species and coke deposition (from TG/DTA) of spent NiRu/TiO<sub>2</sub> catalyst tested in HDO of phenol.

<b>TG/TGA data</b>	NiRu/TiO <sub>2</sub> (calcined)	NiRu/TiO <sub>2</sub> (uncalcined)
Weight gain (%) <sup>a</sup>	2.4	2.8
Weight loss (%) <sup>b</sup>	1.1	0.5 + 0.6

<sup>a</sup> Oxidation of Ni<sup>0</sup> and Ru<sup>0</sup><sup>b</sup> Coke